Molecular Therapy
Original Article

Exosomes from Endothelial Progenitor Cells Improve the Outcome of a Murine Model of Sepsis

Yue Zhou,[1,2] Pengfei Li,[1] Andrew J. Goodwin,[3] James A. Cook,[4] Perry V. Halushka,[5,6] Eugene Chang,[7] and Hongkuan Fan[1,8]

[1]Department of Pathology and Laboratory Medicine, Medical University of South Carolina, Charleston, SC 29425, USA; [2]Department of Biopharmaceutics, College of Pharmacy, Nanjing University of Chinese Medicine, Nanjing 210000, China; [3]Department of Pulmonary, Critical Care, Allergy, and Sleep Medicine, Medical University of South Carolina, Charleston, SC 29425, USA; [4]Department of Neurosciences, Medical University of South Carolina, Charleston, SC 29425, USA; [5]Department of Medicine, Medical University of South Carolina, Charleston, SC 29425, USA; [6]Department of Pharmacology, Medical University of South Carolina, Charleston, SC 29425, USA; [7]Department of Obstetrics-Gynecology, Medical University of South Carolina, Charleston, SC 29425, USA; [8]Department of Regenerative Medicine and Cell Biology, Medical University of South Carolina, Charleston, SC 29425, USA

Microvascular dysfunction leads to multi-organ failure and mortality in sepsis. Our previous studies demonstrated that administration of exogenous endothelial progenitor cells (EPCs) confers protection in sepsis as evidenced by reduced vascular leakage, improved organ function, and increased survival. We hypothesize that EPCs protect the microvasculature through the exosomes-mediated transfer of microRNAs (miRNAs). Mice were rendered septic by cecal ligation and puncture (CLP), and EPC exosomes were administered intravenously at 4 hr after CLP. EPC exosomes treatment improved survival, suppressing lung and renal vascular leakage, and reducing liver and kidney dysfunction in septic mice. EPC exosomes attenuated sepsis-induced increases in plasma levels of cytokines and chemokine. Moreover, we determined miRNA contents of EPC exosomes with next-generation sequencing and found abundant miR-126-3p and 5p. We demonstrated that exosomal miR-126-5p and 3p suppressed LPS-induced high mobility group box 1 (HMGB1) and vascular cell adhesion molecule 1 (VCAM1) levels, respectively, in human microvascular endothelial cells (HMVECs). Inhibition of microRNA-126-5p and 3p through transfection with microRNA-126-5p and 3p inhibitors abrogated the beneficial effect of EPC exosomes. The inhibition of exosomal microRNA-126 failed to block LPS-induced increase in HMGB1 and VCAM1 protein levels in HMVECs and negated the protective effect of exosomes on sepsis survival. Thus, EPC exosomes prevent microvascular dysfunction and improve sepsis outcomes potentially through the delivery of miR-126.

INTRODUCTION

Sepsis is defined as life-threatening organ dysfunction caused by a dysregulated host response to infection.[1–3] Previous studies have shown that microvascular damage occurs early in sepsis and can result in multi-organ dysfunction and ultimately death.[4–7] The endothelium plays a pivotal role in governing microvascular permeability and, thus, regulates organ perfusion and homeostasis.[8] Microvascular injury disrupts endothelial cell tight junctions leading to impaired barrier integrity and activates endothelial cells leading to inflammatory cytokine release and expression of cell adhesion markers.[9,10] These derangements lead to organ edema, local perpetuation of inflammation, and leukocyte trafficking, and play a pivotal role in the development of sepsis-related organ failure.[11,12] Despite this, there are no available pharmacological agents to ameliorate the endothelial dysfunction in sepsis.

Endothelial progenitor cells (EPCs) play a crucial role in maintaining vascular homeostasis and facilitating vascular repair.[13,14] Previous studies by our group as well as others have demonstrated that administration of EPCs have beneficial effects on vascular injury, organ dysfunction, and mortality in a preclinical model of sepsis.[15–17] In addition to repopulating injured endothelium, emerging data suggest that EPCs may also modulate endothelial health through the release of paracrine mediators such as exosomes.[18,19] Exosomes are membranous nanovesicles, 30–120 nm in size, secreted from the endosomal compartment of cells. They mediate intercellular communication via transferring bio-active molecules, including microRNAs (miRNAs). miRNAs are non-coding RNAs that bind to messenger RNAs and inhibit gene expression at the post-transcriptional level. Several studies have suggested that exosomal miRNAs can be taken up by recipient cells with resultant modulation of cellular gene expression and function.[20] Further, recent investigations suggest that miRNAs play a major role in mediating the impact of exosomes on recipient cells[21,22] and have therapeutic potential in endothelial cell dysfunction.[23,24] miR-126, in particular, serves as a crucial regulator of several endothelial cell functions including angiogenesis, vascular repair, inflammatory activation, and apoptosis.[25] Both miR-126-3p and 5p target genes relevant to endothelial activation and inflammation including vascular cell

Received 20 December 2017; accepted 22 February 2018;
https://doi.org/10.1016/j.ymthe.2018.02.020.

Correspondence: Hongkuan Fan, Department of Pathology and Laboratory Medicine, Medical University of South Carolina, 173 Ashley Avenue, MSC 908, CRI Room 610, Charleston, SC 29425, USA.
E-mail: fanhong@musc.edu

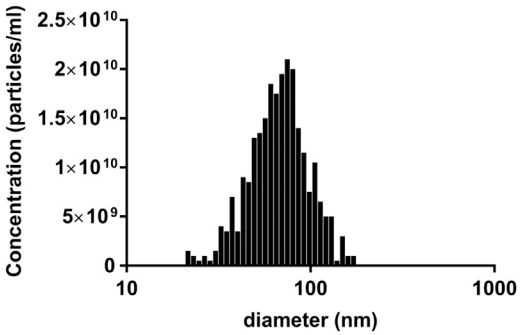

Figure 1. Size Distribution and Total Particle Number of EPC-Exosomes
The number of particles versus particle size was generated by nanoparticle tracking analysis with ZetaView. The results are represented as the mean of three independent experiments.

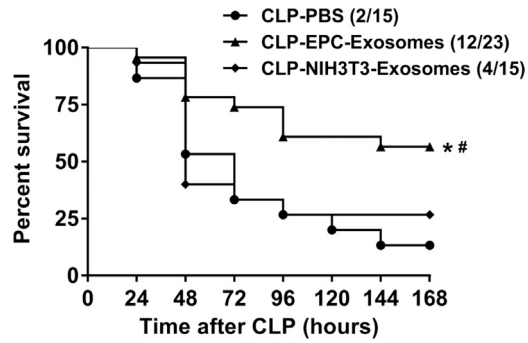

Figure 2. Effect of EPC-Exosomes on CLP-Induced Mortality
CD-1 mice were subjected to CLP and treated with EPC exosomes (2 mg protein/kg body weight), control NIH 3T3-exosomes (2 mg protein/kg body weight), or PBS. Survival rate was monitored for a total of 168 hr (7 days). *$p < 0.05$ compared with CLP-PBS group; #$p < 0.05$ compared with CLP-NIH 3T3-exosomes group. n = 15–23 mice per group.

adhesion molecule 1 (VCAM1) and high mobility group box 1 (HMGB1), respectively.[26–28] However, the role of exosomes and exosomal miR-126-3p and 5p in the microvascular dysfunction of sepsis remains unknown.

We hypothesized that EPC-derived exosomes are beneficial in sepsis and can modulate endothelial cell function, in part, via the transfer of miR-126. In our present study, we investigated the impact of EPC-derived exosomes on survival, organ failure, and inflammation in the cecal ligation and puncture (CLP) model of sepsis. Further, we examined the role of exosomal miR-126 in endothelial activation and sepsis survival. Our results confirmed an important role for exosomal miR-126 in sepsis and suggest that it may represent a potential novel therapeutic option for the treatment of sepsis-induced endothelial cell dysfunction.

RESULTS

EPC-Exosomes Characterization

Human EPCs isolated from cord blood were cultured as previously described.[17] The isolated EPC exosomes were characterized by nanoparticle tracking analysis (NTA) with ZetaView as well as the CD63-based ExoELISA-ULTRA kit (System Bioscience, Palo Alto, CA, USA). We isolated 3.5×10^{10} particles (containing 0.75 mg of exosome protein) from the culture medium of 2.5×10^6 cells with a concentration of 7×10^{10} particles/mL. The average size of exosomes is 71.5 nm, and more than 90% of exosomes are within 30–120 nm range (Figure 1), consistent with previous work.[29]

EPC-Exosome Treatment Improved Survival in CLP-Induced Sepsis

CD-1 mice have been used in our previous studies and are well suited for CLP-induced sepsis.[17] To determine whether EPC exosomes are beneficial, we injected septic mice intravenously with either EPC exosomes (2 mg protein/kg body weight), NIH 3T3-exosomes (2 mg protein/kg body weight), or PBS (control) at 4 hr after CLP surgery. Mouse survival was monitored for 7 days (168 hr). Septic mice treated with EPC exosomes exhibited a significantly increased survival rate compared with mice treated with either NIH 3T3-exosomes or PBS (52% versus 26% and 52% versus 13%, respectively; $p < 0.05$; Figure 2). No significant difference in mortality was observed between NIH 3T3-exosomes and PBS (26% versus 13%; Figure 2).

EPC-Exosomes Attenuated Organ Injury and Vascular Permeability in CLP-Induced Sepsis

Multi-organ dysfunction is a major cause of death during sepsis. We determined whether EPC exosomes improve organ dysfunction in septic mice. Sepsis induced both liver and renal injury as evidenced by the increased aspartate aminotransferase (AST), alanine aminotransferase (ALT), and blood urea nitrogen (BUN) levels in the plasma of septic versus control mice ($p < 0.05$; Figures 3A–3C). However, treatment with EPC exosomes significantly attenuated these organ injuries ($p < 0.05$; Figures 3A–3C). Histologic examination of the sham group revealed normal lung morphology without the presence of infiltrating inflammatory cells (Figure 3D). However, in the CLP group, there were increases in alveolar wall thickening, enlarged interstitial spaces, and alveolar inflammatory cell infiltration consistent with lung injury. These findings were significantly reduced after treatment with EPC exosomes (Figures 3D and 3F). Normal kidney architecture with intact glomeruli, intact brush border of tubular cells, and uniform endothelium were observed in the sham group, but not in the CLP group (Figures 3E and 3G). Treatment with EPC exosomes ameliorated sepsis-related brush border loss, reduced tubular injury, and decreased capillary congestion in the kidney of CLP-induced septic mice (Figures 3E and 3G).

We further investigated the effect of EPC exosomes on vascular leakage and lung edema. CLP mice exhibited a marked increase in lung and kidney vascular leakage assessed by Evans blue tissue dispersion, which were both reversed by EPC exosome treatment ($p < 0.05$; Figures 3H and 3I). Moreover, treatment with EPC exosomes significantly reduced lung water content compared with CLP mice ($p < 0.05$; Figure 3J).

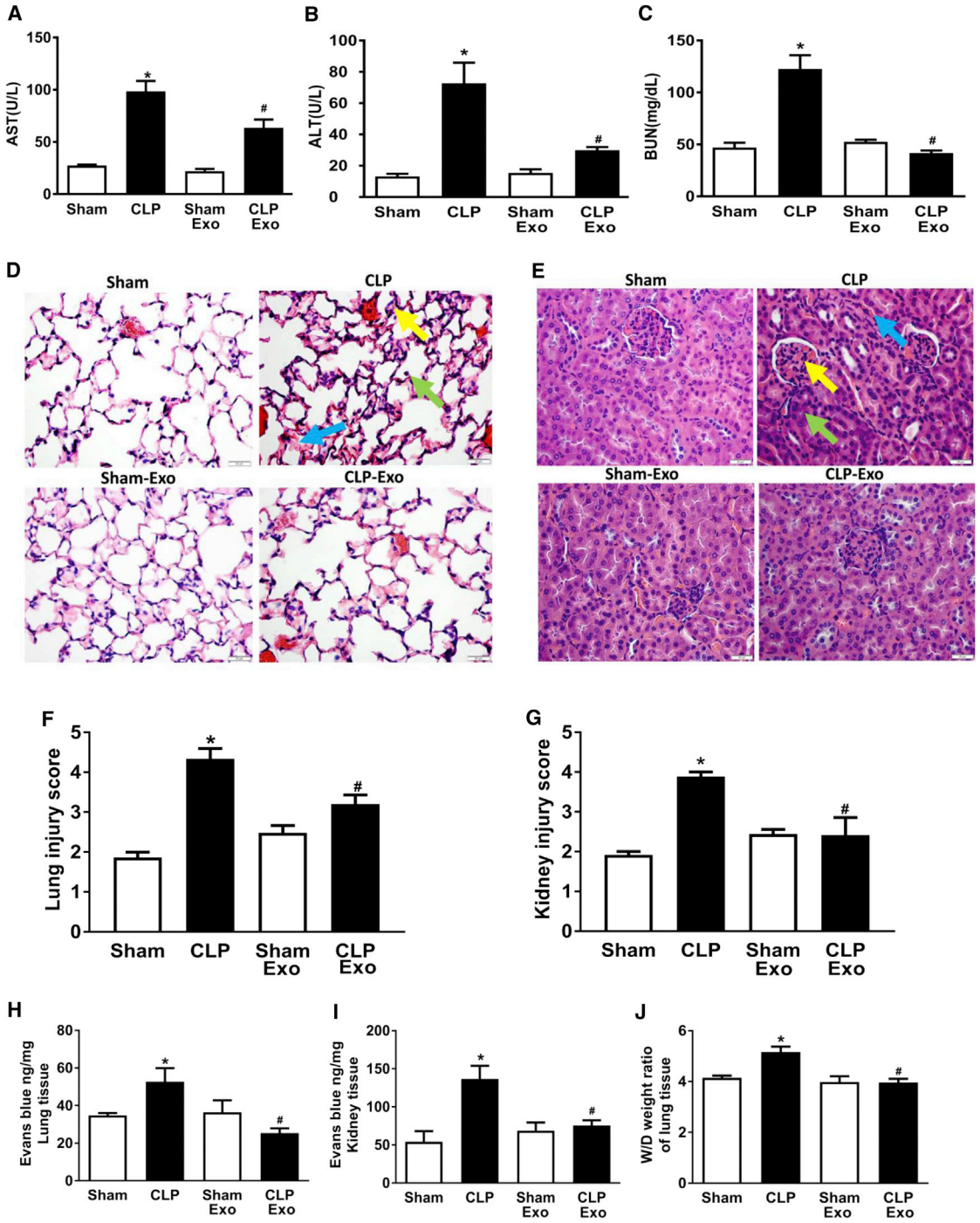

Figure 3. Effect of EPC-Exosomes on Organ Dysfunction, Vascular Leakage, and Lung Edema in CLP-Induced Sepsis

Plasma levels of AST (A), ALT (B), and BUN (C) were measured at 24 hr after CLP. n = 3–6 mice per group. Lung (D) and kidney (E) sections were stained with H&E and examined histologically. The representative sections are shown at ×400 original magnification, and scale bars are 20 μm. For lung histology, the yellow arrow indicates alveolar wall thickening, the green arrow indicates infiltrated inflammatory cells in the alveoli, and the blue arrow indicates enlarged interstitial space. For kidney histology, the yellow arrow indicates a shrunken glomerulus, the green arrow indicates tubular injury including brush border loss and tubular luminal debris or obstruction, and the blue arrow indicates capillary congestion. Lung (F) and renal (G) injury scores were assessed. n = 3–4 mice per group. Vascular leakage in lung (H) and kidney (I) were measured via injecting Evans blue dye at 24 hr after CLP. Lung water content was determined by wet (W)/dry (D) lung tissue weight ratio (J). *$p < 0.05$ compared with the sham group; $^{\#}p < 0.05$ compared with the CLP group. n = 3–6 mice per group. Results are represented as mean ± SE.

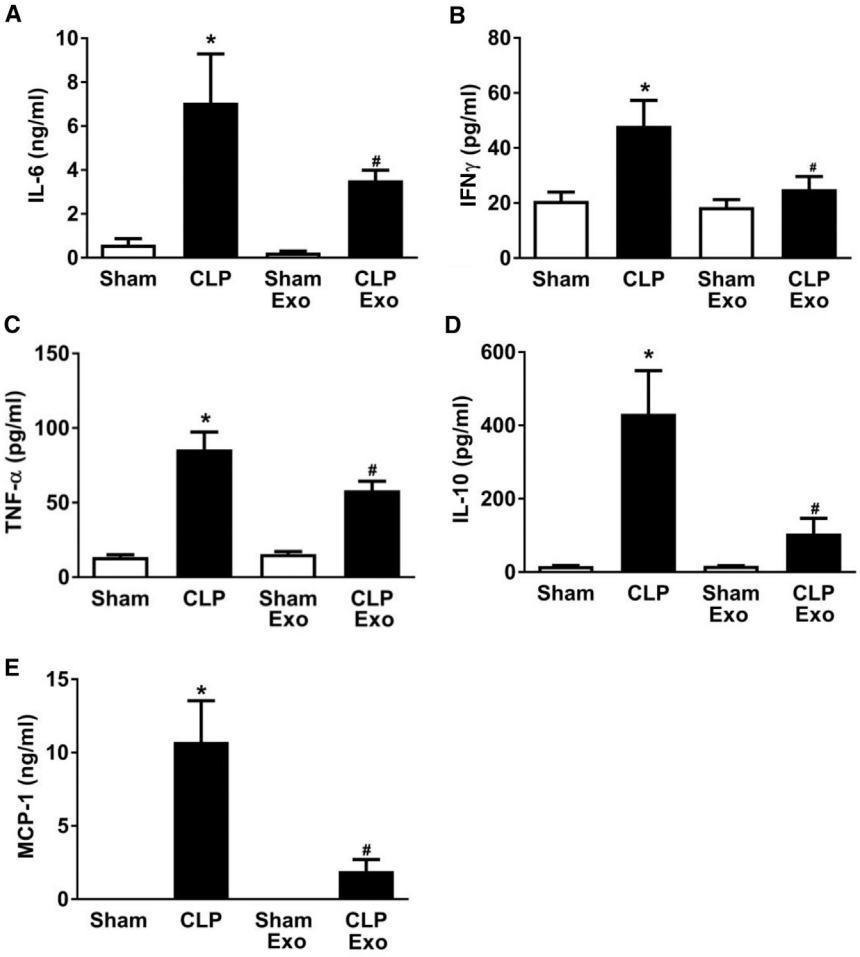

Figure 4. Effect of EPC Exosomes on Plasma Cytokine/Chemokine Levels in Septic Mice

Mice were subjected to sham or CLP and injected with EPC exosomes (2 mg protein/kg body weight) or control PBS (same volume) at 4 hr after CLP surgery. Plasma cytokine IL-6 (A), IFNγ (B), TNF-α (C), IL-10 (D), and chemokine MCP-1 (E) levels were determined by mouse cytokine and chemokine array at 24 hr after CLP. *$p < 0.05$ compared with sham group; #$p < 0.05$ compared with CLP group. n = 3–4 mice per group. Results are represented as mean ± SE.

EPC-Exosomes Reduced Plasma Cytokine/Chemokine Levels in CLP-Induced Sepsis

Sepsis is associated with a systemic inflammatory response driven, in part, by cytokines and chemokines. We determined whether treatment with EPC exosomes had an effect on cytokine and chemokine expression levels in the plasma of septic mice. CLP significantly increased the pro-inflammatory cytokines (interleukin-6 [IL-6], interferon gamma [IFNγ], tumor necrosis factor alpha [TNF-α]) and anti-inflammatory cytokine IL-10, as well as the chemokine MCP-1 ($p < 0.05$; Figure 4). However, treatment with EPC exosomes significantly attenuated these increases ($p < 0.05$; Figure 4).

miR-126-3p and -5p Are Abundantly Expressed in EPC Exosomes

The miRNA contents of EPC and NIH 3T3 cell exosomes were analyzed by next-generation sequencing (NGS) (Tables S1 and S2). Although miR-122-5p was highly expressed in the exosomes from both cells, miR-126-3p and 5p were highly abundant only in EPC exosomes and not in the NIH 3T3-exosomes (Figures 5A and 5B). In combination with the known protective effects of miR-126 on vascular integrity[30–32] and the identical sequences of both murine and human miR-126,[31] this observation led to further investigation of the potential roles of miR-126-3p and 5p in sepsis, and as a potential mediator of our observation that EPC exosomes improve sepsis outcomes.

Treatment with EPC-Exosomes Increased miR-126 and Decreased HMGB1 Expression Level in Lung Tissue

While lung, liver, and kidney fail rapidly during sepsis, we were particularly interested in injury to the lung because exosomes are known to accumulate there,[33,34] and acute lung injury is associated with a high mortality rate in human disease.[35] Because miR-126-3p and 5p are abundant in EPC exosomes, we investigated whether their administration could increase miR-126-3p and 5p expression in the mouse lung using qRT-PCR. Whole lung homogenate was examined 24 hr post-surgery. In both sham-operated and CLP-septic mice, treatment with EPC exosomes significantly augmented miR-126-3p and 5p expression levels compared with untreated mice (Figures 6A and 6B). Furthermore, EPCs-exosome treatment significantly reduced the expression of HMGB1 protein, a known target of miR-126-5p, in lung tissues of septic mice (Figure 6C).

EPC-Exosomes Suppressed Lipopolysaccharide Response in HMVECs through the Delivery of miR-126

We examined the potential mechanism of the beneficial effects of EPC exosomal miRNA-126-3p and 5p by measuring the expression of their targets with established relevance to sepsis, VCAM1, and HMGB1, respectively. Lipopolysaccharide (LPS) increased the protein expression of VCAM1 and HMGB1 in human microvascular endothelial cells (HMVECs), while co-treatment with EPC exosomes mitigated these effects (Figures 7A and 7B). Moreover, reduction of exosomal miR-126-3p and 5p through transfection of EPCs with their inhibitors abrogated these reductions of VCAM1 and HMGB1, respectively (Figures 7A and 7B). Thus, EPC exosomes suppressed LPS-induced increases in VCAM1 and HMGB1 protein levels in part via miR-126-3p and 5p.

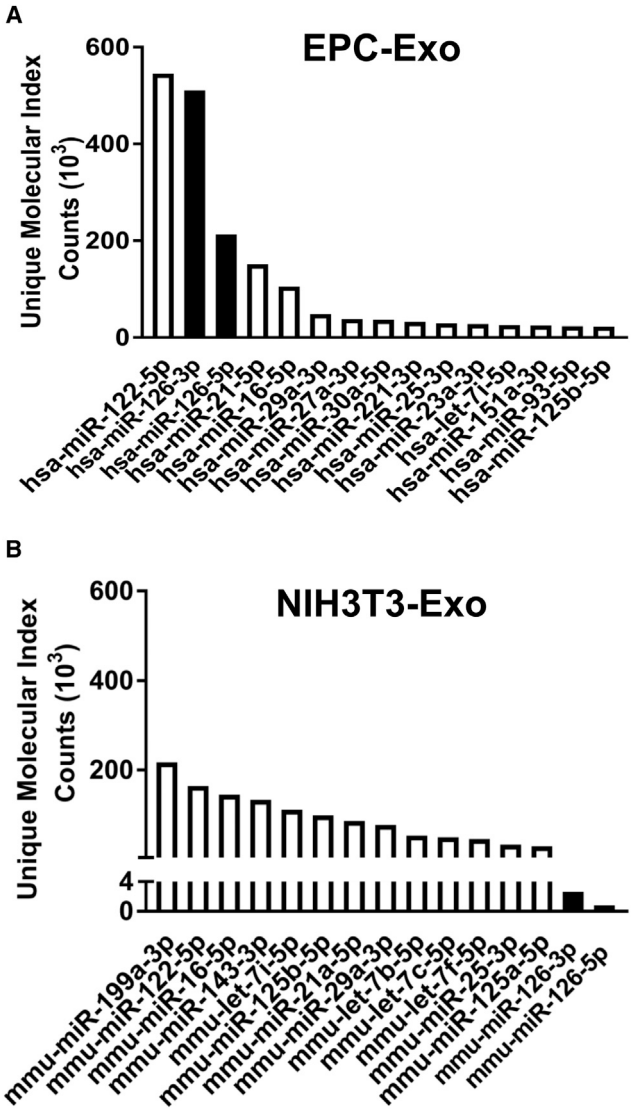

Figure 5. Highly Expressed MicroRNAs Differ between EPC-Exosomes and NIH 3T3 Exosomes

MicroRNA content in EPC exosomes (A) and NIH 3T3 cell exosomes (B) was analyzed by next generation sequencing. Each microRNA expression level was determined by unique molecular index (UMI) from three independent experiments. The results are represented as the mean of three independent experiments.

miRNA-126-Depleted EPC-Exosomes No Longer Improve Sepsis Survival

We lastly determined the potential role of exosomal miR-126 in the survival benefit of EPC exosomes in CLP-induced sepsis. EPC exosome treatment significantly enhanced survival compared with the PBS group (Figure 7C). The group was shown here again for comparison. However, septic mice treated with miR-126-3p- and 5p-depleted EPC exosomes exhibited no significant difference in survival compared with mice treated with PBS (Figure 7C). This suggests that the beneficial effects of EPC exosomes in sepsis are mediated through the delivery of miR-126.

DISCUSSION

In the present study, we found that EPC exosomes impart beneficial effects on microvascular dysfunction in CLP-induced murine sepsis. Treatment with EPC exosomes increased survival, attenuated multiorgan failure, reduced vascular leakage, and suppressed circulating cytokine and chemokine levels. Exosomal delivery of bioactive miRNA to cells is a potential mechanism for these effects, and we identified that miR-126-3p and 5p are highly abundant in EPC exosomes, and their expression is augmented in lung tissue by treatment with these exosomes. Moreover, we demonstrated that EPC exosomes can reduce LPS-induced upregulation of VCAM1 and HMGB1 in endothelial cells through the delivery of miR-126-3p and 5p *in vitro*. Finally, we discovered that EPC exosomes no longer confer a survival benefit in murine sepsis if they are derived from EPCs that have been previously transfected with inhibitors of miR-126-3p and 5p. Taken together, these composite data indicate that EPC exosomes prevent microvascular dysfunction and improve sepsis outcomes potentially through the delivery of miR-126.

In recent years, considerable focus has been given to the potential role of stem or progenitor cells as a therapy for sepsis and its related organ failures.[17,36] While stem cell-based therapy is being examined in early-phase clinical trials,[37,38] the technical challenges involved in scaling up and maintaining stem cell colonies may limit the practical use of this approach. Recent work has suggested that progenitor cells exert their beneficial effects through paracrine mechanisms including through the transmission of mediators via exosomes.[18,19,39] Stem cell- or progenitor cell-derived exosomes possess negligible immunogenicity because, similar to their parent cells, they lack major histocompatibility complex (MHC) class II and co-stimulatory molecules.[40,41] Further, the phospholipid membranes that exosomes inherit are suited to avoid phagocytosis, degradation, and modification in circulation.[42] Thus, stem cell- or progenitor cell-derived exosomes offer a potentially effective and pragmatic approach to novel sepsis therapy development. To our knowledge, the data presented here demonstrate, for the first time, that EPC-derived exosomes mitigate sepsis-related mortality, vascular leak, organ injury, and inflammation possibly through the transfer of protective miR-126 strands to recipient cells, including the endothelium. Future investigations will focus on better understanding the dose-response characteristics, pharmacokinetics, and potential toxicities of EPC exosomes with the intention of ultimately translating this potential therapeutic into early-phase clinical trials in human sepsis.

miRNA-126 is known to play a major role in preservation of endothelial permeability and activation. Through its targeting of Sprouty-related EVH1 Domain 1 (SPRED1) and phosphoinositol-3 kinase regulatory subunit 2 (PIK3R2), miR-126 regulates the endothelial response to vascular endothelial growth factor (VEGF) and its role in endothelial proliferation and permeability.[30] Its importance in vascular integrity has been demonstrated in both zebrafish and

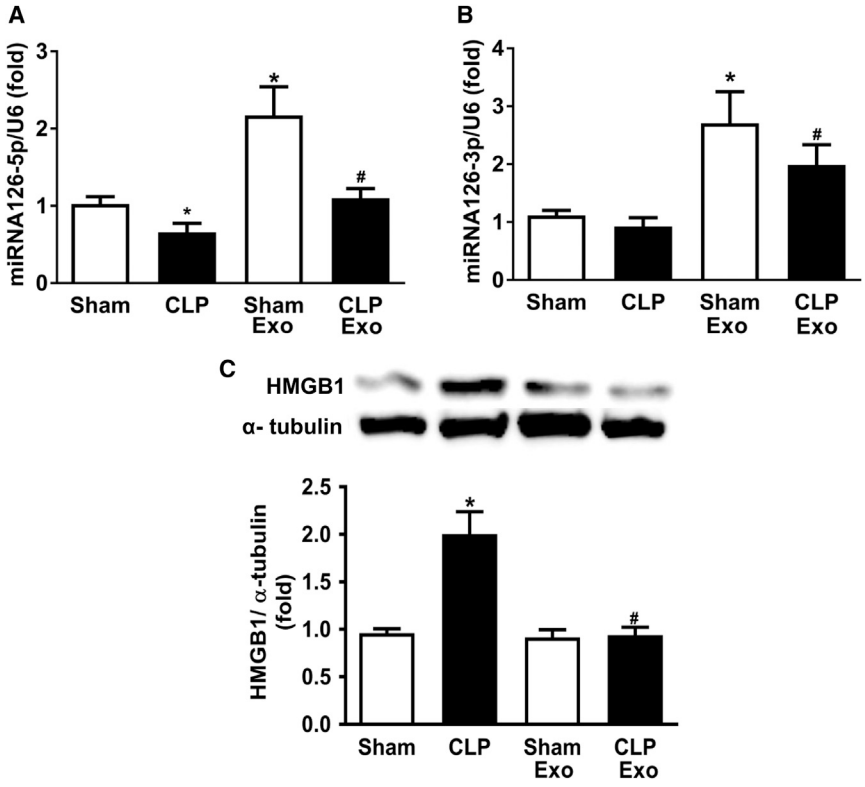

Figure 6. Effect of EPC-Exosomes on miRNA-126-5p and 3p and HMGB1 Protein Levels in Lung Tissue in CLP-Induced Sepsis

Lung miRNA-126-5p (A) and 3p (B) expression were determined by real-time qPCR per group. Protein levels of HMGB1 (C) in lung tissue were measured by western blot. α-Tubulin served as an internal control. *$p < 0.05$ compared with the sham group; #$p < 0.05$ compared with the CLP group. n = 3–6 mice. Results are represented as mean ± SE.

murine models of miR-126 deletion, which demonstrate vascular leak, hemorrhage, and partial embryonic lethality.[30,31] Indeed, miR-126 has been shown to reduce EC barrier disruption by regulating tight junction protein expression including zonula occluden-1 (ZO-1), occludin, and claudin 5.[43] In addition, miR-126 targets and inhibits VCAM1, a key cell adhesion molecule that modulates leukocyte binding to endothelial cells and facilitates leukocyte trafficking into inflamed tissues.[26] More recently, miR-126 was also shown to target and inhibit HMGB1,[28] an inflammatory cytokine known to mediate sepsis pathophysiology and a proposed target for sepsis therapeutics.[44–46] In aggregate, miR-126 inhibits a number of targets that play critical roles in sepsis response pathways including permeability, leukocyte trafficking, and cytokine-mediated inflammation. Our data suggest that EPC-derived exosomes contain abundant miR-126, which can exert paracrine effects on endothelial cells and is, at least in part, responsible for the beneficial effects of these exosomes in sepsis. This is consistent with other disease states where miR-126 has been shown to be a key paracrine mediator promoting endothelial stability.[32]

This study has limitations. First, there were more than 2,300 miRNAs identified in both the EPC- and NIH 3T3-derived exosomes, yet we restricted the focus of this work to miR-126. Although we cannot rule out the possibility that additional miRNAs are also contributing to the beneficial effects of EPC exosomes in sepsis, we assert that our initial focus on miR-126 is justified in the context of its known relevance to endothelial homeostasis and its differential expression in the exosomes from the two cell types. In addition, EPCs-derived microvesicles not only had a beneficial effect on endothelial function,[47] but also protected against ischemia-reperfusion-induced renal injury via miRNA-126.[41] Ongoing bioinformatics analysis may identify additional miRNAs with either beneficial or detrimental effects in sepsis. We also cannot rule out a potential protective effect of other exosomal contents such as lipids or proteins. However, based on our preliminary data, we did not identify potential protective lipids or proteins in EPC exosomes (data not shown). Another limitation is our incomplete understanding of the pharmacokinetics of exosomal therapy. These data provide a proof of concept that EPC exosomes may provide therapeutic benefit in sepsis through the transfer of miRNAs; however, a more thorough understanding of the dose-response relationship and appropriate dosing intervals is required before this could be translated into early-phase clinical trials.

In summary, EPC-derived exosomes represent a promising potential therapy in sepsis. In the murine CLP model, their intravenous delivery improves outcomes including survival and organ injury through the reduction of vascular leak and inflammation. The data presented here suggest that EPC-derived exosomes effectively deliver miRNAs to organs, and that miR-126 may be a critical mediator of their beneficial effects. Ongoing investigation into exosomes and their miRNAs will allow us to better understand their potential as novel sepsis therapeutics.

MATERIALS AND METHODS

Isolation and Characterization of Human EPC Exosomes

Human EPCs isolated from cord blood were cultured as previously described.[17] Cord blood samples were collected from umbilical veins during normal full-term, vaginal deliveries. Informed consent was obtained from the mother for all cord blood collections. This study was approved by the Institutional Review Board for Human Research at the Medical University of South Carolina.

Exosomes were isolated from EPCs and control NIH 3T3 cells culture medium. EPCs were cultured in endothelial basal medium (EBM-2; Lonza, Allendale, NJ, USA) supplemented with EBM-2 SingleQuots

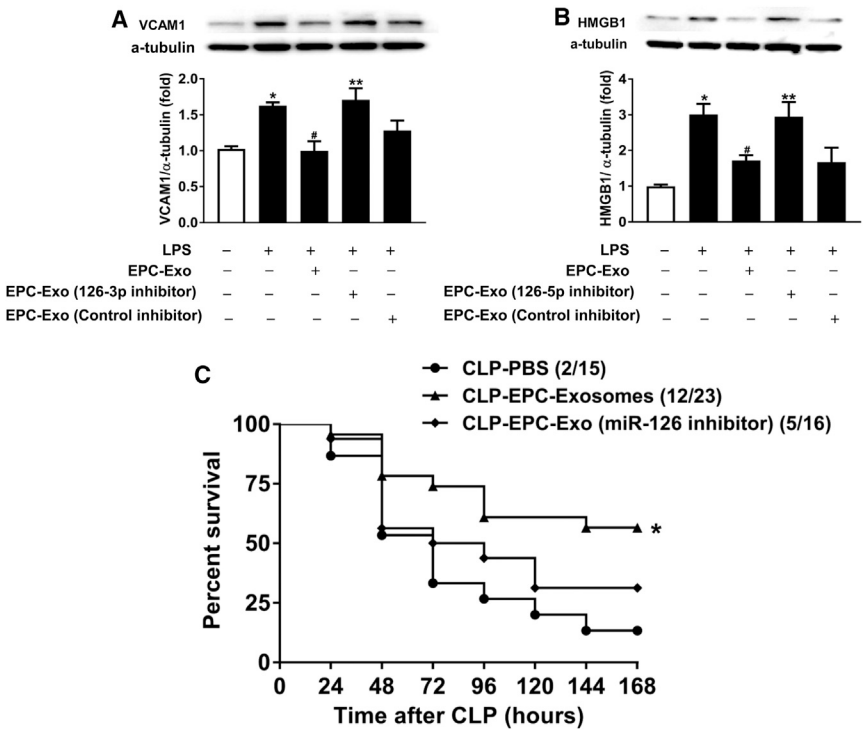

Figure 7. Effect of EPC Exosomal miR-126-3p and 5p on LPS-Induced HMVEC Target Expression and CLP-Induced Mortality

Protein levels of VCAM1 (A) and HMGB1 (B) in HMVECs were measured by western blot. α-Tubulin served as an internal control. *$p < 0.05$ compared with control group; #$p < 0.05$ compared with LPS group; **$p < 0.05$ compared with LPS+ EPC exosomes group. The results represent the means ± SE of three independent experiments. CD-1 mice were subjected to CLP and treated with EPC exosomes, miR-126-reduced EPC exosomes (2 mg protein/kg body weight), or PBS. Survival rate was monitored for a total of 168 hr (7 days) (C). n = 15–16 mice per group.

(Lonza, Allendale, NJ, USA) containing 10% exosome-depleted fetal bovine serum (FBS; System Biosciences, Palo Alto, CA, USA), 1% penicillin and streptomycin (GIBCO, Gaithersburg, MD, USA) for 48 hr, while NIH 3T3 cells were cultured in DMEM medium (GIBCO, Gaithersburg, MD, USA) containing 10% exosome-depleted FBS (System Biosciences, Palo Alto, CA, USA), 1% penicillin and streptomycin (GIBCO, Gaithersburg, MD, USA) for 48 hr before exosome isolation. Medium was harvested and centrifuged at 2,000 × *g* for 30 min to remove cells and debris. Exosomes were then isolated from the cell-free medium using the Total Exosomes Isolation Kit following the manufacturer's instructions (Invitrogen, Asheville, NC, USA) and resuspended in PBS. The total protein concentration of the exosomes was measured by detergent-compatible (DC) protein assay (Bio-Rad, Hercules, CA, USA). Isolated exosomes were diluted in PBS and measured by NTA with ZetaView PMX 120 (Particle Metrix, Meerbusch, Germany). The size distribution and total number of exosomes were analyzed by NTA software (ZetaView 8.04.02). ExoELISA-ULTRA CD63 Kit (System Bioscience, Palo Alto, CA, USA) was also used to quantitate EPC exosome abundance according to the manufacturer's instructions.

Cecal Ligation and Puncture

CD-1 outbred mice (aged 7–8 weeks), which have been used in our previous studies,[17] were housed in a germ-free environment. Investigations conformed to the Guide for the Care and Use of Laboratory Animals published by the NIH and were approved by the Institutional Animal Care and Use Committee at the Medical University of South Carolina. CLP was performed as previously described.[48] In brief, the cecum was ligated at the colon juncture with a 5-0 silk ligature suture without interrupting intestinal continuity and then punctured twice with a 22G needle. All animals were fluid-resuscitated subcutaneously with saline. The sham operation was performed in the same way as CLP except for the ligation and puncture of the cecum.

For the survival study, mice were randomly assigned to one of four groups: sham, CLP-PBS, CLP-EPC exosomes, and CLP-NIH 3T3-Exosomes. At 4 hr after CLP surgery, mice were injected intravenously with PBS, EPC exosomes (2 mg/kg body weight), or NIH 3T3-exosomes (2 mg/kg body weight). The dose was chosen based on our preliminary data and a previous publication.[49] Mice received imipenem (25 mg/kg, subcutaneously) at 6, 24, and 48 hr after CLP, and survival rate was monitored for 7 days.

Organ Function Measurement and Cytokine/Chemokine

Whole blood was collected from mice of each group at 24 hr after surgery and was transferred to a tube containing EDTA (BD Vacutainer, Franklin Lakes, NJ, USA). Plasma was separated by centrifugation at 10,000 rpm for 30 min and stored at −80°C for future analysis.

The plasma levels of ALT, AST, and BUN were used as indicators for liver and kidney function, respectively, and were measured using ELISA kits (BioAssay Systems, Atlanta, GA, USA).

The plasma levels of IL-6, IL-10, TNF-α, IFNγ, and MCP-1 were determined by mouse cytokine and chemokine array pro-inflammatory focused 10-plex, which was performed and analyzed by Eve Technologies (Calgary, AB, Canada).

Lung and Kidney Pathology

The lung and kidney tissues were collected from mice of each *in vivo* group at 48 hr after CLP surgery. The lung tissue was inflated with 10% buffered formalin, and both lung and kidney tissues were fixed with 10% buffered formalin, embedded in paraffin, and cut

into 5-μm sections. Tissue sections were stained with H&E for examination of morphological damage microscopically. At least 10 random lung fields and kidney fields were examined per animal. The lung and kidney injury were evaluated and scored by a pathologist who was blinded to the experimental groups. Lung and kidney injury scores were evaluated as previously described.[50]

Lung and Kidney Vascular Leakage and Lung Wet/Dry Ratio Measurement

Vascular leakage was quantified using the Evans blue dye assay in lung and kidney tissue as described previously.[17] In brief, the mice were administered 1% Evans blue dye solution (Sigma, St. Louis, MO) in saline via tail vein injection. After 40 min, the mice were sacrificed, perfused via the heart and the lung, and kidney tissues were collected. The lung and kidney weights were measured and placed in 1 mL of formamide (Avantor, Center Valley, PA, USA) at 60°C for 24 hr to extract Evans blue dye. The samples were centrifuged at 2,000 rpm for 10 min, and the supernatant was collected. The concentration of Evans blue dye in the supernatant was quantified by measuring absorbance at 620 nm and calculated from a standard curve by a plate reader.

For lung water content, the left lung was harvested and weighed to measure a wet weight in each group. The wet lung was then dried in an oven at 60°C for 48 hr and re-weighed as dry weight. The lung water content was calculated as the ratio of wet weight to dry weight.

miRNA Contents in EPC-Exosomes and NIH 3T3-Exosomes

To determine the miRNA content in EPC and NIH 3T3 exosomes, we examined the miRNA profile by NGS. Total RNA was extracted from 200 μL of EPC exosomes and NIH 3T3-exosomes using the miRNeasy Serum/Plasma Kit (QIAGEN, Germantown, MD, USA) following the manufacturer's instructions. Extracted RNA (100 ng) was used to prepare miRNA-focused NGS libraries using QIAseq miRNA Library Kit (QIAGEN, Germantown, MD, USA). The sequencing was performed on an Illumina HiSeq 2500 instrument at the MUSC Genomic Sequencing Core Facility. The data analysis was performed with the QIAseq miRNA quantification platform using unique molecular index (UMI) counts according to the manufacturer's instructions.

miRNA Inhibitor Transfection

miR-126-3p and 5p inhibitors and a control inhibitor were purchased from QIAGEN. EPCs were cultured and then transfected with miR126-3p or 5p inhibitors (50 nM) or both (25 nM each) or negative control inhibitor (50 nM) using HiPerFect transfection reagent (QIAGEN, Germantown, MD, USA) according to the manufacturer's instruction. Culture medium was replaced with medium containing exosome-depleted FBS (System Biosciences, Palo Alto, CA, USA) at 6 hr after transfection. The exosomes were isolated at 48 hr after transfection as previously described. Isolated exosomes were administered to mice in survival studies as described above and to HMVECs as described below.

HMVECs Culture and Treatment

HMVECs were cultured in EBM-2 (Lonza, Allendale, NJ, USA) supplemented with EGM-2^{MV} SingleQuot (Lonza, Allendale, NJ, USA) containing 5% FBS and 1% penicillin/streptomycin. HMVECs were seeded at 5×10^5 cells/mL with FBS-free culture medium in 12-well plates and treated with exosomes from transfected and untransfected EPCs for 4 hr. Cells were then further stimulated with LPS (100 ng/mL; Sigma, St. Louis, MO, USA) for another 24 hr. The total protein was extracted from cells, and VCAM1 and HMGB1 protein levels were measured by western blot.

Real-Time RT-PCR

Total RNA was extracted from lung tissue using miRNeasy kit (QIAGEN, Germantown, MD, USA) according to the manufacturer's instructions. For miRNA expression, the RNA (12 μL per -reaction) was reverse transcribed using QIAGEN miRNA Reverse Transcription Kit (QIAGEN, Germantown, MD, USA). Following cDNA synthesis, the levels of miRNA 126-3p or 5p were determined by CFX96 Real-Time PCR system (Bio-Rad, Hercules, CA, USA) using SYBR green qPCR master mix (QIAGEN, Germantown, MD, USA) according to the manufacturer's instructions. Data were analyzed with $2^{-\Delta\Delta Ct}$ value calculation, using RNU6 for normalization.

Western Blot

Cells and lung tissues were homogenized and lysed with ice-cold radioimmunoprecipitation assay (RIPA) lysis buffer (Abcam, Cambridge, MA, USA) containing protease and phosphatase inhibitors (Cell Signaling, Boston, MA, USA). All lysed samples were kept on ice for 30 min and centrifuged for 10 min at 4°C at 10,000 × *g*. The cell lysate was collected and protein concentration was measured using a DC protein assay (Bio-Rad, Hercules, CA, USA). Fifty micrograms of protein was used for western blot analysis. Primary antibodies including anti-HMGB1 (1:1,000; Cell Signaling, Boston, MA, USA) and anti-VCAM1 (1:500; Cell Signaling, Boston, MA, USA) were used. Peroxidase-labeled anti-rabbit antibody (GE Healthcare, Pittsburgh, PA, USA) was used as secondary antibody. α-Tubulin (1:1000; Cell Signaling, Boston, MA) was used as a loading control. The immunoreactive protein bands were visualized by ECL detection kit (GE Healthcare, Pittsburgh, PA, USA) and analyzed using ImageJ software.

Statistical Analysis

The *in vitro* experiments were performed at least three independent times. The data were analyzed using GraphPad Prism 7.01 software and are represented as mean ± SE. The log rank test was used for comparisons in the survival study, while analysis of variance with the Fisher probable least-squares difference test was used for other comparisons. A value of $p < 0.05$ was considered statistically significant.

SUPPLEMENTAL INFORMATION

Supplemental Information includes two tables and can be found with this article online at https://doi.org/10.1016/j.ymthe.2018.02.020.

AUTHOR CONTRIBUTIONS

Conception and design: H.F., Y.Z., P.L., A.J.G., P.V.H., J.A.C. Acquisition of data, or analysis and interpretation of data: Y.Z., H.F., P.L., A.J.G., P.V.H., J.A.C., E.C. Drafting the article: Y.Z, H.F., A.J.G., P.L., P.V.H., J.A.C.

CONFLICTS OF INTEREST

The authors declare no conflict of interest.

ACKNOWLEDGMENTS

We thank Dr. Lixia Zhang and Dr. Russell A. Harley for their histologic evaluations. This work was supported in part by NIGMS grants 1R01GM113995 (to H.F. and P.V.H.), 1K23HL135263-01A1 (to A.J.G.), and UL1TR001450 (to P.V.H.) and the Genomics Shared Resource Center, Hollings Cancer Center, Medical University of South Carolina (P30 CA138313).

REFERENCES

1. Freund, Y., Lemachatti, N., Krastinova, E., Van Laer, M., Claessens, Y.E., Avondo, A., Occelli, C., Feral-Pierssens, A.L., Truchot, J., Ortega, M., et al.; French Society of Emergency Medicine Collaborators Group (2017). Prognostic accuracy of sepsis-3 criteria for in-hospital mortality among patients with suspected infection presenting to the emergency department. JAMA *317*, 301–308.

2. Shankar-Hari, M., Phillips, G.S., Levy, M.L., Seymour, C.W., Liu, V.X., Deutschman, C.S., Angus, D.C., Rubenfeld, G.D., and Singer, M.; Sepsis Definitions Task Force (2016). Developing a new definition and assessing new clinical criteria for septic shock: for the Third International Consensus Definitions for Sepsis and Septic Shock (Sepsis-3). JAMA *315*, 775–787.

3. Rudd, K.E., Delaney, A., and Finfer, S. (2017). Counting sepsis, an imprecise but improving science. JAMA *318*, 1228–1229.

4. Doerschug, K.C., Delsing, A.S., Schmidt, G.A., and Haynes, W.G. (2007). Impairments in microvascular reactivity are related to organ failure in human sepsis. Am. J. Physiol. Heart Circ. Physiol. *293*, H1065–H1071.

5. Gill, S.E., Rohan, M., and Mehta, S. (2015). Role of pulmonary microvascular endothelial cell apoptosis in murine sepsis-induced lung injury in vivo. Respir. Res. *16*, 109.

6. Wang, L., Mehta, S., Brock, M., and Gill, S.E. (2017). Inhibition of murine pulmonary microvascular endothelial cell apoptosis promotes recovery of barrier function under septic conditions. Mediators Inflamm. *2017*, 3415380.

7. Vincent, J.L., and De Backer, D. (2005). Microvascular dysfunction as a cause of organ dysfunction in severe sepsis. Crit. Care *9* (*Suppl 4*), S9–S12.

8. Aird, W.C. (2003). The role of the endothelium in severe sepsis and multiple organ dysfunction syndrome. Blood *101*, 3765–3777.

9. David, S., Thamm, K., Schmidt, B.M.W., Falk, C.S., and Kielstein, J.T. (2017). Effect of extracorporeal cytokine removal on vascular barrier function in a septic shock patient. J. Intensive Care *5*, 12.

10. Rho, S.S., Ando, K., and Fukuhara, S. (2017). Dynamic regulation of vascular permeability by vascular endothelial cadherin-mediated endothelial cell-cell junctions. J. Nippon Med. Sch. *84*, 148–159.

11. London, N.R., Zhu, W., Bozza, F.A., Smith, M.C., Greif, D.M., Sorensen, L.K., Chen, L., Kaminoh, Y., Chan, A.C., Passi, S.F., et al. (2010). Targeting Robo4-dependent Slit signaling to survive the cytokine storm in sepsis and influenza. Sci. Transl. Med. *2*, 23ra19.

12. Trzeciak, S., Dellinger, R.P., Parrillo, J.E., Guglielmi, M., Bajaj, J., Abate, N.L., Arnold, R.C., Colilla, S., Zanotti, S., and Hollenberg, S.M.; Microcirculatory Alterations in Resuscitation and Shock Investigators (2007). Early microcirculatory perfusion derangements in patients with severe sepsis and septic shock: relationship to hemodynamics, oxygen transport, and survival. Ann. Emerg. Med. *49*, 88–98, e1–2.

13. Iwaguro, H., Yamaguchi, J., Kalka, C., Murasawa, S., Masuda, H., Hayashi, S., Silver, M., Li, T., Isner, J.M., and Asahara, T. (2002). Endothelial progenitor cell vascular endothelial growth factor gene transfer for vascular regeneration. Circulation *105*, 732–738.

14. Kalka, C., Masuda, H., Takahashi, T., Kalka-Moll, W.M., Silver, M., Kearney, M., Li, T., Isner, J.M., and Asahara, T. (2000). Transplantation of ex vivo expanded endothelial progenitor cells for therapeutic neovascularization. Proc. Natl. Acad. Sci. USA *97*, 3422–3427.

15. Xu, X., Yang, J., Li, N., Wu, R., Tian, H., Song, H., and Wang, H. (2015). Role of endothelial progenitor cell transplantation in rats with sepsis. Transplant. Proc. *47*, 2991–3001.

16. Güldner, A., Maron-Gutierrez, T., Abreu, S.C., Xisto, D.G., Senegaglia, A.C., Barcelos, P.R., Silva, J.D., Brofman, P., de Abreu, M.G., and Rocco, P.R. (2015). Expanded endothelial progenitor cells mitigate lung injury in septic mice. Stem Cell Res. Ther. *6*, 230.

17. Fan, H., Goodwin, A.J., Chang, E., Zingarelli, B., Borg, K., Guan, S., Halushka, P.V., and Cook, J.A. (2014). Endothelial progenitor cells and a stromal cell-derived factor-1α analogue synergistically improve survival in sepsis. Am. J. Respir. Crit. Care Med. *189*, 1509–1519.

18. Li, X., Chen, C., Wei, L., Li, Q., Niu, X., Xu, Y., Wang, Y., and Zhao, J. (2016). Exosomes derived from endothelial progenitor cells attenuate vascular repair and accelerate reendothelialization by enhancing endothelial function. Cytotherapy *18*, 253–262.

19. Zhang, J., Chen, C., Hu, B., Niu, X., Liu, X., Zhang, G., Zhang, C., Li, Q., and Wang, Y. (2016). Exosomes derived from human endothelial progenitor cells accelerate cutaneous wound healing by promoting angiogenesis through Erk1/2 signaling. Int. J. Biol. Sci. *12*, 1472–1487.

20. Zhang, J., Li, S., Li, L., Li, M., Guo, C., Yao, J., and Mi, S. (2015). Exosome and exosomal microRNA: trafficking, sorting, and function. Genomics Proteomics Bioinformatics *13*, 17–24.

21. Squadrito, M.L., Baer, C., Burdet, F., Maderna, C., Gilfillan, G.D., Lyle, R., Ibberson, M., and De Palma, M. (2014). Endogenous RNAs modulate microRNA sorting to exosomes and transfer to acceptor cells. Cell Rep. *8*, 1432–1446.

22. Guduric-Fuchs, J., O'Connor, A., Camp, B., O'Neill, C.L., Medina, R.J., and Simpson, D.A. (2012). Selective extracellular vesicle-mediated export of an overlapping set of microRNAs from multiple cell types. BMC Genomics *13*, 357.

23. Umezu, T., Ohyashiki, K., Kuroda, M., and Ohyashiki, J.H. (2013). Leukemia cell to endothelial cell communication via exosomal miRNAs. Oncogene *32*, 2747–2755.

24. Umezu, T., Tadokoro, H., Azuma, K., Yoshizawa, S., Ohyashiki, K., and Ohyashiki, J.H. (2014). Exosomal miR-135b shed from hypoxic multiple myeloma cells enhances angiogenesis by targeting factor-inhibiting HIF-1. Blood *124*, 3748–3757.

25. Chistiakov, D.A., Orekhov, A.N., and Bobryshev, Y.V. (2016). The role of miR-126 in embryonic angiogenesis, adult vascular homeostasis, and vascular repair and its alterations in atherosclerotic disease. J. Mol. Cell. Cardiol. *97*, 47–55.

26. Harris, T.A., Yamakuchi, M., Ferlito, M., Mendell, J.T., and Lowenstein, C.J. (2008). MicroRNA-126 regulates endothelial expression of vascular cell adhesion molecule 1. Proc. Natl. Acad. Sci. USA *105*, 1516–1521.

27. Chu, M., Qin, S., Wu, R., Zhou, X., Tang, X., Zhang, S., Zhao, Q., Wang, H., Liu, Y., Han, X., et al. (2016). Role of MiR-126a-3p in Endothelial Injury in Endotoxic Mice. Crit. Care Med. *44*, e639–e650.

28. Tang, S.T., Wang, F., Shao, M., Wang, Y., and Zhu, H.Q. (2017). MicroRNA-126 suppresses inflammation in endothelial cells under hyperglycemic condition by targeting HMGB1. Vascul. Pharmacol. *88*, 48–55.

29. Helwa, I., Cai, J., Drewry, M.D., Zimmerman, A., Dinkins, M.B., Khaled, M.L., Seremwe, M., Dismuke, W.M., Bieberich, E., Stamer, W.D., et al. (2017). A comparative study of serum exosome isolation using differential ultracentrifugation and three commercial reagents. PLoS ONE *12*, e0170628.

30. Fish, J.E., Santoro, M.M., Morton, S.U., Yu, S., Yeh, R.F., Wythe, J.D., Ivey, K.N., Bruneau, B.G., Stainier, D.Y., and Srivastava, D. (2008). miR-126 regulates angiogenic signaling and vascular integrity. Dev. Cell *15*, 272–284.

31. Wang, S., Aurora, A.B., Johnson, B.A., Qi, X., McAnally, J., Hill, J.A., Richardson, J.A., Bassel-Duby, R., and Olson, E.N. (2008). The endothelial-specific microRNA miR-126 governs vascular integrity and angiogenesis. Dev. Cell *15*, 261–271.

32. Zernecke, A., Bidzhekov, K., Noels, H., Shagdarsuren, E., Gan, L., Denecke, B., Hristov, M., Köppel, T., Jahantigh, M.N., Lutgens, E., et al. (2009). Delivery of microRNA-126 by apoptotic bodies induces CXCL12-dependent vascular protection. Sci. Signal. *2*, ra81.

33. Takahashi, Y., Nishikawa, M., Shinotsuka, H., Matsui, Y., Ohara, S., Imai, T., and Takakura, Y. (2013). Visualization and in vivo tracking of the exosomes of murine melanoma B16-BL6 cells in mice after intravenous injection. J. Biotechnol. *165*, 77–84.

34. Imai, T., Takahashi, Y., Nishikawa, M., Kato, K., Morishita, M., Yamashita, T., Matsumoto, A., Charoenviriyakul, C., and Takakura, Y. (2015). Macrophage-dependent clearance of systemically administered B16BL6-derived exosomes from the blood circulation in mice. J. Extracell. Vesicles *4*, 26238.

35. Yeh, L.C., Huang, P.W., Hsieh, K.H., Wang, C.H., Kao, Y.K., Lin, T.H., and Lee, X.L. (2017). Elevated plasma levels of Gas6 are associated with acute lung injury in patients with severe sepsis. Tohoku J. Exp. Med. *243*, 187–193.

36. Keane, C., Jerkic, M., and Laffey, J.G. (2017). Stem cell-based therapies for sepsis. Anesthesiology *127*, 1017–1034.

37. Matthay, M.A. (2015). Therapeutic potential of mesenchymal stromal cells for acute respiratory distress syndrome. Ann. Am. Thorac. Soc. *12* (*Suppl 1*), S54–S57.

38. Wilson, J.G., Liu, K.D., Zhuo, H., Caballero, L., McMillan, M., Fang, X., Cosgrove, K., Vojnik, R., Calfee, C.S., Lee, J.W., et al. (2015). Mesenchymal stem (stromal) cells for treatment of ARDS: a phase 1 clinical trial. Lancet Respir. Med. *3*, 24–32.

39. Yue, Y., Garikipati, V.N.S., Verma, S.K., Goukassian, D.A., and Kishore, R. (2017). Interleukin-10 deficiency impairs reparative properties of bone marrow-derived endothelial progenitor cell exosomes. Tissue Eng. Part A *23*, 1241–1250.

40. Le Blanc, K., Tammik, C., Rosendahl, K., Zetterberg, E., and Ringdén, O. (2003). HLA expression and immunologic properties of differentiated and undifferentiated mesenchymal stem cells. Exp. Hematol. *31*, 890–896.

41. Cantaluppi, V., Gatti, S., Medica, D., Figliolini, F., Bruno, S., Deregibus, M.C., Sordi, A., Biancone, L., Tetta, C., and Camussi, G. (2012). Microvesicles derived from endothelial progenitor cells protect the kidney from ischemia-reperfusion injury by microRNA-dependent reprogramming of resident renal cells. Kidney Int. *82*, 412–427.

42. Laulagnier, K., Motta, C., Hamdi, S., Roy, S., Fauvelle, F., Pageaux, J.F., Kobayashi, T., Salles, J.P., Perret, B., Bonnerot, C., and Record, M. (2004). Mast cell- and dendritic cell-derived exosomes display a specific lipid composition and an unusual membrane organization. Biochem. J. *380*, 161–171.

43. Zhuang, Y., Peng, H., Mastej, V., and Chen, W. (2016). MicroRNA regulation of endothelial junction proteins and clinical consequence. Mediators Inflamm. *2016*, 5078627.

44. Wang, H., Bloom, O., Zhang, M., Vishnubhakat, J.M., Ombrellino, M., Che, J., Frazier, A., Yang, H., Ivanova, S., Borovikova, L., et al. (1999). HMG-1 as a late mediator of endotoxin lethality in mice. Science *285*, 248–251.

45. Yang, H., Ochani, M., Li, J., Qiang, X., Tanovic, M., Harris, H.E., Susarla, S.M., Ulloa, L., Wang, H., DiRaimo, R., et al. (2004). Reversing established sepsis with antagonists of endogenous high-mobility group box 1. Proc. Natl. Acad. Sci. USA *101*, 296–301.

46. Suda, K., Kitagawa, Y., Ozawa, S., Saikawa, Y., Ueda, M., Ebina, M., Yamada, S., Hashimoto, S., Fukata, S., Abraham, E., et al. (2006). Anti-high-mobility group box chromosomal protein 1 antibodies improve survival of rats with sepsis. World J. Surg. *30*, 1755–1762.

47. Deregibus, M.C., Cantaluppi, V., Calogero, R., Lo Iacono, M., Tetta, C., Biancone, L., Bruno, S., Bussolati, B., and Camussi, G. (2007). Endothelial progenitor cell derived microvesicles activate an angiogenic program in endothelial cells by a horizontal transfer of mRNA. Blood *110*, 2440–2448.

48. Fan, H., Bitto, A., Zingarelli, B., Luttrell, L.M., Borg, K., Halushka, P.V., and Cook, J.A. (2010). Beta-arrestin 2 negatively regulates sepsis-induced inflammation. Immunology *130*, 344–351.

49. Wang, X., Gu, H., Qin, D., Yang, L., Huang, W., Essandoh, K., Wang, Y., Caldwell, C.C., Peng, T., Zingarelli, B., and Fan, G.C. (2015). Exosomal miR-223 contributes to mesenchymal stem cell-elicited cardioprotection in polymicrobial sepsis. Sci. Rep. *5*, 13721.

50. Li, H., Wang, S., Zhan, B., He, W., Chu, L., Qiu, D., Li, N., Wan, Y., Zhang, H., Chen, X., et al. (2017). Therapeutic effect of Schistosoma japonicum cystatin on bacterial sepsis in mice. Parasit. Vectors *10*, 222.

YMTHE, Volume *26*

Supplemental Information

Exosomes from Endothelial Progenitor Cells Improve the Outcome of a Murine Model of Sepsis

Yue Zhou, Pengfei Li, Andrew J. Goodwin, James A. Cook, Perry V. Halushka, Eugene Chang, and Hongkuan Fan

Table S1 Top 160 MicroRNAs in EPC-exosomes by Next Generation Sequencing

Rank	miRNA	UMIs	Rank	miRNA	UMIs
1	hsa-miR-122-5p	545004.67	41	hsa-let-7f-5p	5938.00
2	hsa-miR-126-3p	510846.67	42	hsa-miR-451a	5593.00
3	hsa-miR-126-5p	213417.00	43	hsa-let-7a-5p	5451.00
4	hsa-miR-21-5p	151090.33	44	hsa-miR-29c-3p	5315.00
5	hsa-miR-16-5p	105002.67	45	hsa-miR-369-3p	5101.00
6	hsa-miR-29a-3p	48160.00	46	hsa-miR-320a	5082.33
7	hsa-miR-27a-3p	38231.00	47	hsa-miR-101-3p	5019.00
8	hsa-miR-30a-5p	36556.33	48	hsa-miR-222-3p	4870.33
9	hsa-miR-221-3p	32306.33	49	hsa-miR-199b-3p	4746.33
10	hsa-miR-25-3p	29207.67	50	hsa-miR-320c	4725.67
11	hsa-miR-23a-3p	27513.67	51	hsa-miR-30e-5p	4561.33
12	hsa-let-7i-5p	25748.67	52	hsa-miR-30d-5p	4440.67
13	hsa-miR-151a-3p	24980.67	53	hsa-miR-134-5p	4393.33
14	hsa-miR-93-5p	23405.00	54	hsa-miR-130a-3p	3996.67
15	hsa-miR-125b-5p	22758.67	55	hsa-miR-361-5p	3984.00
16	hsa-miR-24-3p	17827.33	56	hsa-miR-26a-5p	3925.67
17	hsa-let-7b-5p	17188.00	57	hsa-miR-660-5p	3841.67
18	hsa-miR-10b-5p	15044.33	58	hsa-miR-186-5p	3566.00
19	hsa-miR-92a-3p	14688.67	59	hsa-let-7c-5p	3471.33
20	hsa-miR-199a-3p	14003.67	60	hsa-miR-17-5p	3362.67
21	hsa-miR-432-5p	11401.67	61	hsa-miR-217	3243.67
22	hsa-miR-191-5p	11082.33	62	hsa-miR-148b-3p	3232.00
23	hsa-miR-148a-3p	10809.33	63	hsa-miR-335-5p	3187.33
24	hsa-miR-27b-3p	10436.33	64	hsa-miR-31-5p	3115.00
25	hsa-miR-22-3p	10289.00	65	hsa-miR-424-5p	2951.00
26	hsa-miR-100-5p	10191.00	66	hsa-miR-192-5p	2935.00
27	hsa-miR-146a-5p	10177.00	67	hsa-miR-99a-5p	2903.33
28	hsa-miR-10a-5p	9736.33	68	hsa-miR-20a-5p	2872.67
29	hsa-miR-127-3p	9203.67	69	hsa-miR-181b-5p	2847.67
30	hsa-miR-423-5p	8895.00	70	hsa-miR-103a-3p	2821.00
31	hsa-miR-409-3p	8318.33	71	hsa-miR-125a-5p	2815.67
32	hsa-miR-155-5p	7925.33	72	hsa-miR-378a-3p	2739.33
33	hsa-miR-34a-5p	7663.33	73	hsa-miR-494-3p	2666.00
34	hsa-miR-19b-3p	7303.00	74	hsa-miR-510-3p	2639.67
35	hsa-miR-28-3p	6625.33	75	hsa-miR-145-5p	2587.67
36	hsa-miR-152-3p	6556.00	76	hsa-miR-654-3p	2553.67
37	hsa-miR-382-5p	6195.33	77	hsa-miR-142-5p	2518.67
38	hsa-miR-133a-3p	6026.67	78	hsa-miR-140-3p	2450.00
39	hsa-miR-128-3p	5991.67	79	hsa-miR-30c-5p	2445.33
40	hsa-miR-380-3p	5963.00	80	hsa-miR-381-3p	2433.00

Rank	miRNA	UMIs	Rank	miRNA	UMIs
81	hsa-miR-26b-5p	2432.67	121	hsa-miR-29b-3p	1001.00
82	hsa-miR-365b-3p	2374.67	122	hsa-miR-19a-3p	996.67
83	hsa-miR-15a-5p	2353.33	123	hsa-miR-889-3p	974.00
84	hsa-miR-1246	2319.67	124	hsa-let-7d-3p	954.33
85	hsa-miR-130b-3p	2306.00	125	hsa-miR-382-3p	948.00
86	hsa-miR-486-5p	2267.00	126	hsa-miR-10a-3p	875.00
87	hsa-miR-7-5p	2214.33	127	hsa-miR-154-5p	852.33
88	hsa-miR-376a-3p	2148.67	128	hsa-miR-214-3p	852.00
89	hsa-let-7e-5p	2070.00	129	hsa-miR-142-3p	821.67
90	hsa-miR-532-5p	2062.00	130	hsa-miR-299-5p	771.67
91	hsa-miR-181a-5p	1996.00	131	hsa-miR-487b-3p	766.33
92	hsa-miR-30a-3p	1855.00	132	hsa-miR-499a-5p	747.00
93	hsa-miR-136-3p	1853.00	133	hsa-miR-485-3p	713.33
94	hsa-miR-143-3p	1801.67	134	hsa-miR-337-5p	684.67
95	hsa-miR-185-5p	1798.33	135	hsa-miR-206	678.33
96	hsa-miR-15b-5p	1778.67	136	hsa-miR-365a-3p	676.33
97	hsa-miR-376c-3p	1723.00	137	hsa-miR-425-5p	658.00
98	hsa-miR-196b-5p	1707.33	138	hsa-miR-345-5p	655.00
99	hsa-miR-320b	1675.67	139	hsa-miR-374a-5p	637.00
100	hsa-miR-99b-5p	1653.67	140	hsa-miR-584-5p	631.33
101	hsa-miR-574-3p	1617.67	141	hsa-miR-197-3p	626.67
102	hsa-miR-379-5p	1580.33	142	hsa-miR-18a-5p	623.33
103	hsa-miR-107	1538.00	143	hsa-miR-337-3p	604.00
104	hsa-miR-216a-5p	1404.33	144	hsa-miR-361-3p	591.67
105	hsa-miR-224-5p	1346.33	145	hsa-miR-369-5p	557.00
106	hsa-miR-137	1321.33	146	hsa-miR-378c	533.33
107	hsa-miR-6817-3p	1316.33	147	hsa-miR-3976	529.00
108	hsa-miR-345-3p	1256.00	148	hsa-miR-455-5p	521.33
109	hsa-miR-503-5p	1223.67	149	hsa-miR-193a-5p	516.00
110	hsa-miR-323a-3p	1196.00	150	hsa-miR-10b-3p	513.33
111	hsa-miR-629-5p	1191.00	151	hsa-miR-625-3p	511.33
112	hsa-miR-411-5p	1170.67	152	hsa-miR-99b-3p	498.67
113	hsa-miR-1307-3p	1167.33	153	hsa-miR-21-3p	487.00
114	hsa-let-7g-5p	1161.67	154	hsa-miR-421	485.00
115	hsa-miR-423-3p	1160.67	155	hsa-miR-218-5p	483.00
116	hsa-miR-574-5p	1156.33	156	hsa-miR-23b-3p	481.33
117	hsa-miR-194-5p	1148.33	157	hsa-miR-484	480.00
118	hsa-miR-339-5p	1102.00	158	hsa-miR-450b-5p	479.00
119	hsa-miR-151b/151a-5p	1067.33	159	hsa-miR-320d	471.00
120	hsa-miR-342-3p	1045.00	160	hsa-miR-199a-5p	454.00

Table S2 Top 160 microRNAs in NIH3T3-exosome by Next Generation Sequencing

Rank	miRNA	UMIs	Rank	miRNA	UMIs
1	mmu-miR-199a/b-3p	216507.33	41	mmu-miR-409-3p	7759.33
2	mmu-miR-122-5p	164033.67	42	mmu-miR-19b-3p	7736.33
3	mmu-miR-16-5p	144452.33	43	mmu-miR-26b-5p	7536.67
4	mmu-miR-143-3p	132905.67	44	mmu-miR-22-3p	7293.33
5	mmu-let-7i-5p	111383.00	45	mmu-miR-130a-3p	7253.00
6	mmu-miR-125b-5p	98648.33	46	mmu-miR-92a-3p	6308.33
7	mmu-miR-21a-5p	85768.00	47	mmu-miR-345-3p	6305.67
8	mmu-miR-29a-3p	77377.33	48	mmu-miR-206-3p	6245.67
9	mmu-let-7b-5p	53210.00	49	mmu-miR-101b-3p	6087.33
10	mmu-let-7c-5p	49610.33	50	mmu-miR-29b-3p	6077.67
11	mmu-let-7f-5p	45343.00	51	mmu-miR-183-5p	5802.33
12	mmu-miR-25-3p	32673.67	52	mmu-miR-411-5p	5799.33
13	mmu-miR-125a-5p	29558.67	53	mmu-miR-300-3p	5637.33
14	mmu-let-7e-5p	28015.00	54	mmu-miR-378a-3p	5631.33
15	mmu-miR-27a-3p	27760.33	55	mmu-miR-127-3p	5150.00
16	mmu-miR-23a-3p	26542.33	56	mmu-miR-30c-5p	5097.00
17	mmu-miR-93-5p	26371.00	57	mmu-miR-100-5p	4429.00
18	mmu-miR-382-5p	24404.67	58	mmu-miR-103-3p	4388.67
19	mmu-miR-31-5p	23632.33	59	mmu-miR-186-5p	4236.67
20	mmu-miR-99b-5p	22320.33	60	mmu-miR-28a-3p	4210.67
21	mmu-let-7a-5p	19912.67	61	mmu-miR-146b-5p	4210.33
22	mmu-miR-182-5p	19381.33	62	mmu-miR-214-3p	3738.67
23	mmu-miR-152-3p	18523.00	63	mmu-miR-34a-5p	3665.00
24	mmu-miR-140-3p	17232.33	64	mmu-miR-29c-3p	3629.00
25	mmu-miR-30a-5p	16717.67	65	mmu-miR-342-3p	3498.67
26	mmu-miR-379-5p	16020.00	66	mmu-miR-218-5p	3390.00
27	mmu-miR-7a-5p	15534.67	67	mmu-miR-532-5p	3344.33
28	mmu-miR-30d-5p	14889.00	68	mmu-miR-10a-5p	3297.33
29	mmu-miR-26a-5p	13011.00	69	mmu-let-7g-5p	3079.00
30	mmu-miR-24-3p	12524.00	70	mmu-let-7d-5p	3052.00
31	mmu-miR-221-3p	12123.00	71	mmu-miR-9-5p	2955.33
32	mmu-miR-134-5p	11435.67	72	mmu-miR-542-3p	2813.67
33	mmu-miR-322-5p	10853.33	73	mmu-miR-148a-3p	2783.33
34	mmu-miR-30e-5p	10087.33	74	mmu-miR-423-5p	2753.00
35	mmu-miR-10b-5p	9751.67	75	mmu-miR-365-3p	2739.67
36	mmu-miR-541-5p	9680.67	76	mmu-miR-320-3p	2714.00
37	mmu-miR-191-5p	9524.00	77	mmu-miR-17-5p	2640.67
38	mmu-miR-145a-5p	9219.67	78	mmu-miR-126a-3p	2635.67
39	mmu-miR-27b-3p	8727.33	79	mmu-miR-154-5p	2463.67
40	mmu-miR-199a-5p	8622.33	80	mmu-miR-101a-3p	2324.67

Rank	miRNA	UMIs	Rank	miRNA	UMIs
81	mmu-miR-494-3p	2201.33	121	mmu-miR-30e-3p	965.00
82	mmu-miR-15b-5p	2198.67	122	mmu-miR-107-3p	955.67
83	mmu-let-7d-3p	2197.00	123	mmu-miR-142a-3p	951.00
84	mmu-miR-30b-5p	2152.00	124	mmu-miR-185-5p	945.00
85	mmu-miR-503-5p	2139.67	125	mmu-miR-19a-3p	940.67
86	mmu-miR-148b-3p	2104.00	126	mmu-miR-376b-3p	940.33
87	mmu-miR-299a-3p	2080.00	127	mmu-miR-486b-5p	897.00
88	mmu-miR-155-5p	1941.00	128	mmu-miR-31-3p	880.67
89	mmu-miR-99b-3p	1891.00	129	mmu-miR-98-5p	868.67
90	mmu-miR-351-5p	1835.33	130	mmu-miR-744-5p	853.00
91	mmu-miR-381-3p	1824.33	131	mmu-miR-151-3p	806.00
92	mmu-miR-34c-5p	1818.00	132	mmu-miR-126a-5p	794.00
93	mmu-miR-140-5p	1792.00	133	mmu-miR-425-5p	739.00
94	mmu-miR-30a-3p	1719.00	134	mmu-miR-872-3p	702.67
95	mmu-miR-299b-3p	1681.33	135	mmu-miR-15a-5p	695.33
96	mmu-miR-128-3p	1678.67	136	mmu-miR-432	689.00
97	mmu-miR-222-3p	1592.67	137	mmu-miR-485-3p	680.00
98	mmu-miR-298-5p	1576.00	138	mmu-miR-434-5p	671.33
99	mmu-miR-1839-5p	1508.33	139	mmu-miR-671-5p	639.00
100	mmu-miR-674-5p	1473.67	140	mmu-miR-143-5p	638.67
101	mmu-miR-361-5p	1413.33	141	mmu-miR-199b-5p	635.00
102	mmu-miR-615-3p	1372.33	142	mmu-miR-328-3p	617.33
103	mmu-miR-20a-5p	1361.67	143	mmu-miR-181a-5p	602.67
104	mmu-miR-296-3p	1338.00	144	mmu-miR-3074-5p	597.00
105	mmu-miR-125b-1-3p	1331.67	145	mmu-miR-421-3p	590.33
106	mmu-miR-133a-3p	1313.67	146	mmu-miR-125a-3p	585.33
107	mmu-miR-151-5p	1294.67	147	mmu-miR-1198-5p	581.67
108	mmu-miR-872-5p	1264.67	148	mmu-let-7a-1/7c-2-3p	565.33
109	mmu-miR-192-5p	1247.67	149	mmu-miR-34b-3p	564.00
110	mmu-miR-301a-3p	1225.67	150	mmu-miR-299a-5p	562.33
111	mmu-miR-23b-3p	1216.67	151	mmu-miR-106b-3p	552.67
112	mmu-miR-350-3p	1183.67	152	mmu-miR-434-3p	540.33
113	mmu-miR-210-3p	1127.00	153	mmu-miR-329-5p	538.33
114	mmu-miR-369-3p	1091.33	154	mmu-miR-376a-3p	534.00
115	mmu-miR-130b-3p	1037.00	155	mmu-miR-129-5p	530.33
116	mmu-miR-451a	1026.00	156	mmu-miR-335-5p	518.00
117	mmu-miR-574-5p	1006.33	157	mmu-miR-15b-3p	502.33
118	mmu-miR-196a-5p	1006.00	158	mmu-miR-1983	500.33
119	mmu-miR-574-3p	976.67	159	mmu-miR-652-3p	496.33
120	mmu-miR-99a-5p	973.00	160	mmu-let-7b-3p	483.33